Convective heat transfer on leeward building walls in an urban environment: measurements in an outdoor scale model

A. Nottrott[*], S. Onomura[†], A. Inagaki[†], M. Kanda[†] and J. Kleissl[*‡]

[*]University of California, San Diego
Department of Mechanical and Aerospace Engineering
La Jolla, California, USA

[†]Tokyo Institute of Technology
Department of International Development Engineering
Tokyo, Japan

[‡]*Corresponding author*
University of California, San Diego
Department of Mechanical and Aerospace Engineering
9500 Gilman Drive
EBU II Building
La Jolla, CA 92093-0411, USA
Tel.: +1 858 534 8087
Fax: +1 858 534 7599
Email: jkleissl@ucsd.edu

Abstract

Convection over the building envelope is a critical determinant of building cooling load, but parameterization of convection in building energy models and urban computational fluid dynamics models is challenging. An experimental investigation intended to clarify the heat transfer mechanism of a convective wall boundary layer (WBL) on a leeward, vertical building wall was conducted at the Comprehensive Outdoor Scale Model (COSMO) facility for urban atmospheric research. By comparing profiles of mean temperature and turbulent temperature fluctuation intensity we determined that the dominant regime of the WBL flow was turbulent natural convection. Continuous wavelet transform analysis was applied to detect intermittent turbulent natural and forced convection events in the WBL. Implications for parameterization of convective heat fluxes in urban areas are discussed.

Keywords: boundary layer; convection; sensible heat flux; urban; vertical wall; wall function.

Nomenclature

C_g	wavelet coefficient
d	momentum thickness
f_n	characteristic frequency of temperature timeseries
Gr_x, Gr_H	local and average Grashof number
g	gravitational acceleration
H	building roof height
h_o	external surface to air convection coefficient
L	Obukhov length
Nu_x, Nu_H	local and average Nusselt number
Q_H	sensible heat flux at the wall
Re_x, Re_H	local and average Reynolds number
Ri	flux Richardson number
S	distance between buildings
T	temperature
U_*	friction velocity
U,V,W	streamwise, spanwise and vertical velocity components for the COSMO model
u,v,w	streamwise and spanwise velocity components for the wall boundary layer
X,Y,Z	coordinate system for the COSMO model
x,y,z	coordinate system for the wall boundary layer
Z_{eff}	effective measurement height due to flow displacement by buildings.

Greek symbols

β	coefficient of volume expansion
ζ	dimensionless wall coordinate for the wall boundary layer
θ	dimensionless temperature
λ	thermal conductivity of fluid
ν	kinematic viscosity of fluid
ξ	atmospheric stability parameter
σ	standard deviation
φ	wavelet scaling function
ψ	wavelet function.

Superscript

‘	denotes a time dependent variable with zero mean (fluctuating component)
^	variable in frequency space (Fourier transform).

Subscript

eff	effective
f	film
tr	turbulent transition
S	wall surface condition
∞	free stream (ambient) condition.

Symbols

<>	denotes time averaged quantity.

1. Introduction

Coupled meteorological and engineering models that incorporate numerical simulations of atmospheric turbulence are needed to accurately quantify turbulent heat and passive scalar transport in urban environments [1]. Sensible heat flux *(Q_H)* is a critical component of the urban energy balance and impacts building cooling load [2]. Q_H is driven by fine-scale turbulence of O(cm) in wall boundary layers (WBL) on urban surfaces located within the roughness sublayer (RSL) of the atmospheric surface layer over urban areas. However, existing urban atmospheric

models frequently have computational domains of size O(km) and cannot accurately simulate turbulent structures (and implicitly Q_H) in WBLs, because the computational cost required to resolve turbulent fluid motions, let alone viscous layers, in the WBL is prohibitive [3], [4]. In order to accurately model Q_H over urban surfaces it is necessary to apply simplified convection models called wall functions (WF) which estimate the surface to air convection coefficient (h_o) in $Q_H = h_o(T_s - T_\infty)$.

Turbulence and heat flux in convective WBLs on a vertically oriented flat plate have been studied extensively with indoor experiments. Cheesewright [5], [6] studied mean velocity and temperature profiles and heat transfer in laminar, transitional and turbulent natural convective BLs. Tsuji & Nagano [7] reported the first turbulence measurements that fully resolved the viscous region in a vertical turbulent natural convection WBL in water channel experiments. Turbulence characteristics and the structure of a vertical turbulent combined convection WBL were investigated and visualized by Kitamura & Inagaki [8]. They observed a decrease in local convective heat flux between the wall and the free stream with increasing local Reynolds number (Re_x) of the free stream (up to the combined-forced convection transition). Hattori et al. [9], [10] measured velocity and temperature in a turbulent combined convection WBL along a vertical heated plate with a free stream flow in a vertical wind tunnel. Hattori et al. classified different regimes of the flow based on the local Grashof (Gr_x) and Reynolds numbers and observed suppressed heat transfer in combined-convection which they attributed to re-laminarization of the turbulent free convection BL under the influence of an aiding free stream.Numerical experiments [11], [12] and [13] have employed different turbulence models to investigate the various flow regimes of vertical WBL convection. Patel et al [13] used a low turbulence Reynolds number k-ε model [14] to develop flow regime classifications similar to Kitamura & Inagaki [8] and Hattori et al [9]. Patel et al found that the transition to turbulence occurred at similar Re_x ($10^5 < Re_{x,tr} < 10^6$) and smaller Gr_x ($10^{8.5} < Gr_{x,tr} < 10^{9.5}$) than observed by Hattori et al and they clarified the range of Gr_x and Re_x for the turbulent combined convection regime.

Existing WFs for Q_H on vertical walls of full-scale buildings were primarily derived from spatially averaged measurements of heat flux parameters assuming a steady state energy balance over the measurement surface area. Nusselt-Jürges type correlations [15] of the form $h_0 = AV + B$ are used to relate h_o to a representative wind speed measurement V through empirical constants A and B. For example, Hagishima & Tanimoto [16] correlated h_o and the near wall wind

velocity for windward and leeward vertical walls of a 2.4 m cubic test dwelling mounted on the roof of a four story building. Henmi et al [17] developed similar correlations from data collected on an exposed wall of a full-scale, residential building. Loveday & Taki [2] also made measurements on a full-scale building, but they correlated h_o with rooftop wind speed. Many WFs of this type exist and are reviewed extensively in Cole & Sturrock [18] and Palyvos [19].

All of these models have limitations that make their application as WFs in urban boundary layer models problematic. Wind tunnel and water channel experiments have low turbulence intensities in the free stream unlike the real atmospheric surface layer which is highly turbulent and unsteady. Consequently the transition to turbulence in outdoor WBLs is expected to occur much earlier than in wind tunnel experiments, because the transition is sensitive to turbulence levels in the free stream (as in bypass transition [20]). Numerical simulations of turbulent convective WBLs are idealized and the transition to turbulence must be prescribed in the model from empirical values of $Gr_{x,tr}$ and $Re_{x,tr}$ [13]. The primary shortcoming of energy balance based WFs (i.e. WFs that infer h_o from measurements of net radiation and conduction) is that they are derived from average heat flux parameters. Data to calibrate energy balance based WFs are often measured in complex urban environments and lack broad applicability [19].

The goal of this study is to examine the thermal structure of the WBL and improve understanding of the mechanism for convection on leeward walls of buildings in dense urban areas. In the present study the building height to separation ratio is $H/S = 1.0$. Heat transfer on leeward walls in dense urban areas is unique due to the flow structure that develops in the urban canyon (UC). At side walls, the velocity speed up due to channelling effects in UCs oriented parallel to the streamwise direction of the mean wind favours forced convection. The wind speed at leeward building walls is expected to be smaller than at the roof or side walls, because of wake formation in the lee of the building, which favours natural convection. However, in UCs oriented normal to the streamwise direction of the mean wind, a canyon vortex (cavity eddy) develops in the UC which generates a mean flow that is directed upward along the leeward wall, and is parallel to the buoyant force acting on air parcels heated at the wall [21]. Thus one might expect that the heat transfer mechanism on leeward walls is combined convection.

Many authors have investigated the flow structure and heat flux around building-like roughness elements in full-scale cities and scaled outdoor and wind tunnel models. The flow structure around an isolated wall-mounted cube as well as multiple obstacle configurations, in

fully-developed turbulent channel flow, has been studied extensively using qualitative flow visualization and quantitative velocimetry techniques [22], [23]. Those and many other results were collated by [24]. Onomura et al. [25] used particle image velocimetry (PIV) and sonic anemometry in a 1/5 scale, outdoor urban model (refer to section 2.1) to study the effect of heated vertical walls (with various orientations relative to the prevailing wind) on the flow structure in the urban canyon (UC). However, the WBLs in the UC were not resolved due to performance limitations of the PIV system.

Knowledge of the heat transfer regime in the WBL will be useful for developing WFs that are universally applicable to urban environments. For the first time we report outdoor turbulence measurements of temperature in the WBL and velocity in and above the UC in the lee of a model building at the Comprehensive Outdoor Scale MOdel (COSMO) of an urban area. It is worth noting that experimental studies of atmospheric dynamics in an urban-like environment were conducted at the outdoor scale model Mock Urban Setting Test (MUST) facility in Utah, U.S.A. [26]. To the knowledge of the authors, none of the MUST experiments investigated turbulence and sensible heat flux in vertical WBLs.

Perhaps the most thorough study of local sensible heat flux on a vertical wall in an urban-like setting was executed by Meinders [24], [27]. Meinders measured the velocity field around a wall-mounted cube array inside a wind tunnel and the spatial variability of convective heat flux on the walls of a single heated cube. Meinders observed large gradients in h_o across the vertical faces of the cube. Unfortunately because Meinders' experiment was designed to study cooling of electronics, the inflow conditions and boundary conditions were not comparable to the present experiment.

This article is structured in the following manner: In Section 2 we describe the COSMO facility, the experimental setup and provide theoretical background relevant to the analysis. In Section 3 we characterize the analysis periods chosen for detailed study. Sections 4 and 5 present the results and discussion respectively.

2. Experiment design

2.1 COSMO facility

The COSMO facility at the Nippon Institute of Technology in Saitama, Japan is a 1/5 scale model of an urban residential area specifically designed to study urban atmospheric and energy transport processes. The model consists of a 100 m by 50 m concrete foundation and 512 model buildings (Fig. 1). The model buildings are hollow, concrete cubes with height H = 1.5 m. The cubes are arranged on a regular grid so that the building to model plan area ratio is 1/4. The buildings are spaced by S = 1.5 m (H/S = 1.0). The predominant wind direction is from the SE so that the NW-SE axis of COSMO becomes the streamwise axis for the flow above the COSMO model. For further description of the COSMO facility see [28].

Separate coordinate systems are defined for the COSMO model and the WBL. The coordinate system relative to the COSMO model (X,Y,Z are streamwise, spanwise, and vertical direction given flow above the canopy, respectively) has the origin at ground level on the 'x' in Fig. 1. The velocities associated with this coordinate frame are (U,V,W). For the WBL coordinates (x,y), the x-axis lies along the vertical centre-line of the building wall with the origin on the ground and the x coordinate (streamwise direction) increasing with height above the concrete foundation. The y-axis is normal to wall and the y coordinate is zero on the wall and increases positively away from the surface (see Fig. 2). The velocities associated with the WBL coordinate frame are (u,v). For simplicity the WBL is approximated as two dimensional and turbulence statistics are assumed to be homogeneous in the z direction (spanwise direction).

2.2 Experiment setup

The experiment was setup near the centre of COSMO on the NE-SW axis (see Fig. 1) so that the streamwise fetch was 50 m for SE winds. Turbulence in the mean flow was assumed to be spatially homogeneous at a height of $2H$ based on the measurements of Inagaki & Kanda [28]. Applying the definition for the RSL proposed by Cheng & Castro [29] the height $2H$ is considered to be outside the RSL for COSMO based on the spatial convergence of horizontal turbulence statistics.

The experimental setup (Fig. 2) consisted of three sonic anemometers mounted in and above the UC. Two fine-wire thermocouple rakes, that measured profiles of temperature and temperature fluctuations in the WBL, were fixed at two heights along the centre-line of the

model building wall ($x = 0.67H$ and $0.90H$) and temperature measurements were made along a line parallel to the y-axis. Each thermocouple rake had 15 Type E, fine-wire thermocouples with a junction wire diameter of 0.03 mm arranged in an approximately logarithmic spacing from the wall. Additional thermocouples were attached to the building wall with conductive tape and measured wall surface temperature at the base of both thermocouple rakes. Three dimensional turbulent wind velocity measurements were made using three KAIJO DA-600 sonic anemometers mounted at several locations on a 4 m mast. One anemometer was mounted in the UC between the thermocouple rakes at (x,y) =($0.78H$, 150 mm) and measured the velocity near the building wall. Two sonic anemometers mounted above the buildings (at $Z = 1.22H$ and $2H$) were used to measure the velocities outside the RSL and atmospheric stability. All instruments were sampled continuously at 50 Hz.

An Eko, ISO 9060 Second Class thermopile pyranometer measured global horizontal irradiance (*GHI*) above the buildings (at $Z = 2H$) since radiation from the sun is the primary heat input to the system. Irradiance data from the pyranometer were sampled at 1 Hz and averaged and stored once per minute along with the intra-minute standard deviation of irradiance σ_{GHI}.

2.3 Relevant scales

Velocity and length scales are defined in terms of reference wind velocity measurements and COSMO dimensions. The wind speed at height $Z = 2H$ is used as the velocity scale for the surface layer $(U^2+V^2)^{1/2}$. The free stream velocity scale for the WBL u_∞ is taken to be the vertical component of the velocity measured by the lowest sonic anemometer at (x,y) =($0.78H$, 150 mm) (see Fig. 2). Usually the distance along the x-axis from the origin is taken as the length scale for the local Grashof, Reynolds and Nusselt numbers (Gr_x, Re_x and Nu_x). The local dimensionless numbers are defined as

$$Gr_x = \frac{g\beta(T_S - T_\infty)x^3}{\nu^2}, \quad (1a)$$

$$Re_x = \frac{u_\infty x}{\nu}, \quad (1b)$$

$$Nu_x = \frac{h_o x}{\lambda}, \quad (1c)$$

where g is the gravitational acceleration, $\beta = 1/T_\infty$ is the coefficient of volume expansion, ν is the kinematic viscosity and λ is the thermal conductivity of the fluid. Fluid properties are taken at the mean film temperature $\langle T_f \rangle = (\langle T_S \rangle + \langle T_\infty \rangle)/2$, where $\langle T_S \rangle$ and $\langle T_\infty \rangle$ are the average wall temperature and free stream temperatures respectively at $x = 0.67H$, $0.9H$ and $y = 150$ mm.

Both temperature and relative humidity were large in the near wall region so the properties of dry air were not applicable to this analysis. The psychrometric model of Tsilingiris [30] was applied to compute the thermophysical and transport properties of moist air for heat transfer calculations. In our situation the starting location of the WBL is not obvious because the ground presents a barrier to the flow in x direction. For this reason we use the building wall height as the length scale for the local dimensionless groups (Gr_H, Re_H and Nu_H). Although the choice of H as the length scale is not consistent with boundary layer scaling in simpler geometries, it provides a relevant scaling parameter.

The dimensionless temperature variable θ is obtained by scaling temperature measurements in the WBL by $<T_S>$ and $<T_\infty>$ such that $\theta = (T - <T_\infty>)/(<T_S> - <T_\infty>)$, where angle brackets denote a time average.

2.4 Classification of Heat Transfer Regime

Previous studies mapped the heat transfer regimes of the WBL on an isothermal heated wall with uniform surface temperature as a function of Gr_x and Re_x. Fig. 3a is the map of heat transfer regimes generated by Patel et al [13] over a wide range of Gr_x and Re_x ($10 \leq Gr_x < 10^{13}$ and $10 \leq Re_x < 10^7$). The range of Gr_x and Re_x encountered in this experiment is small since it was not possible to control meteorological conditions, but the dimensionless numbers in the present study are representative of real urban areas (albeit at 1/5 scale). Fig. 3a indicates that the flow should become fully turbulent for $Gr_x > 5.0x10^9$ which suggests that the WBL flow regime observed in COSMO should be transitional combined convection. Fig. 3b is the flow regime map developed by Hattori et al [9] from experiments in a vertical wind tunnel with minimal turbulence in the free stream, i.e. $\sigma_u/u_\infty < 1.6\%$ and $\sigma_v/u_\infty < 0.8\%$. Hattori et al [9] mapped convection regimes over the range $5x10^7 \leq Gr_x < 10^{13}$ and $5x10^2 \leq Re_x < 10^8$, but their map is different than that of Patel et al. The laminar region in Hattori et al extends to the upper limit of their experiments ($Gr_x = 3.58x10^{11}$) because they observed complete re-laminarization of a turbulent natural convection WBL in the presence of an aiding free stream. Based on the Hattori et al map the regime of the WBL flow observed in COSMO should be laminar combined convection. These classifications of the WBL flow are inconsistent motivating further study of convective WBLs on buildings.

3. Analysis periods

Three day-long experimental campaigns were carried out in COSMO during July 2010. The raw data was filtered in order to obtain continuous 30 min datasets. Constant Gr_H was obtained by requiring stationarity for the wall surface temperature variance ($\sigma_{Ts}^2 < 0.4$ K^2) and the canyon air temperature variance ($\sigma_{T\infty}^2 < 1$ K^2) during the 30 min period. The air temperature variance is expected to be larger than the wall temperature variance due to advection and thermal inertia effects. After these conditions were applied two 30 minute data sets remained for this analysis. Temperature data were conditioned before analysis to eliminate noise and remove long term trends. High frequency noise was removed with a high frequency cut-off ($f_c > 11.53$ Hz) and detrending was accomplished by filtering out all frequency content $f < 0.001$ Hz corresponding to the lowest frequencies present in the data as recommended by Frasier et al [31].

Atmospheric stability ξ was estimated as

$$\xi = \frac{Z_{eff}}{L} = \frac{-(g/\langle T\rangle)\langle W'T'\rangle}{U_*^3/(\lambda Z_{eff})}, \quad (2)$$

where L is the Obukhov length and Z_{eff} is the effective measurement height defined as the difference between the actual measurement height (Z) and the momentum thickness d, which is the effective origin of the Z axis because the flow in the atmospheric surface layer is displaced by the model buildings in COSMO [28]. The value d = 1.3 m is calculated using the correlations developed by Thom [32]. The friction velocity is defined in terms of the Reynolds stress as $U_* = (\langle U'W'\rangle)^{1/2}$ and T is the air temperature. In stability calculations both U_* and T are measured above the RSL at $Z = 2H$. Mean values of ξ for each 30-min run are listed in Table 1 along with the mean flux Richardson number (Ri).

$$Ri = \frac{(g/\langle T\rangle)\langle W'T'\rangle}{\langle U'W'\rangle\frac{\partial\langle U\rangle}{\partial z} + \langle V'W'\rangle\frac{\partial\langle V\rangle}{\partial z}} \quad (3)$$

In Eqs. 2 and 3 primes denote fluctuations obtained from Reynolds decomposition. Values of ξ and Ri represent the stability of atmospheric thermal stratification. Neutral stability corresponds to $\xi = Ri = 0$, so both qualified data sets can be characterized as weakly unstable.

4. Results

4.1 Flow in the urban canyon

Correlation of wind speed measurements in and above the RSL confirmed the existence of a re-circulating eddy in the UC. Fig. 4 shows the relationship between the mean surface layer wind speed (height *2H*) and the vertical velocity near the leeward building wall. The mean vertical velocity (u_∞) at the leeward wall is always positive indicating re-circulating flow about the *Y* axis. $<u_\infty>$ increases with $<U^2+V^2>^{1/2}$ which shows that the strength of the cavity eddy in the UC is linked to the wind speed above the street canyon. The magnitude of the standard deviation of u_∞ is much larger than $<u_\infty>$ which indicates that although the mean flow in the UC is re-circulating, turbulent velocity fluctuations in the canyon flow are much stronger than the mean flow. These findings are consistent with the experiments of Louka et al [33] who found that the typical mean flow in an UC is characterized by a re-circulating eddy and that the strength of the eddy is coupled to the wind speed outside the RSL.

If a persistent re-circulation in the UC exists, the BL flow on leeward building walls can be approximated as natural convection from a vertical flat plate with an aiding free stream flow (i.e. the gravity field is parallel and opposite the free stream vertical velocity near the wall). Such flows were discussed in Section 1 and data from those experiments provide the primary basis for comparison with our measurements.

4.2 Mean profiles of temperature and temperature standard deviation

Determination of the WBL flow regime using the maps in Fig. 3 was inconclusive so we attempt to classify the flow based on the thermal structure of the WBL. In this section dimensionless profiles of mean temperature and turbulent temperature fluctuations from the vertical, heated, leeward building wall in COSMO are compared with data from wind tunnel and water channel experiments of turbulent natural convection along a vertical heated plate with uniform wall surface temperature $T_S = const.$ [7], [34] and constant temperature difference between the surface and the free stream along the streamwise direction $T_S - T_\infty = const.$ [35]. Figure 5a shows established mean temperature profiles for a turbulent natural convection WBL and profiles from the present study plotted as a function of the length parameter $\zeta = (y/x)Nu_x = -y(\partial\theta/\partial y)|_{y=0}$ (not to be confused with the atmospheric stability parameter ξ). The temperature gradient at the wall $\partial\theta/\partial y|_{y=0}$ (which is proportional to the convective heat flux) was

approximated from the slope between the wall temperature and the temperature measurement nearest the wall in the WBL, i.e. *[θ(y=0* mm*) – θ(y=1.2* mm*)]/(1.2* mm*)* (see section 5 for further discussion). Good agreement is observed between the data in the range $0.3<\zeta<10$. Scatter between the data in the free stream region $\zeta>10$ does not necessarily indicate a discrepancy between the measurements because the shape of the temperature profile near the free stream depends on the choice of location for the free stream reference temperature (refer to definition of θ in Section 2.3). The near wall region ($\zeta<0.3$) was not resolved in the present study so no comparison was possible there, but we note that existing data (Fig. 5a) indicate that the slope of the temperature profile varies significantly in this region (refer to section 5).Profiles of turbulent temperature standard deviation from Tsuji & Nagano [7] are plotted with data from the present study in Fig. 5b. Acceptable agreement between the data is observed in the range $0.3<\zeta<3$. In the outer region of the WBL near the free stream ($\zeta>3$) the intensity of turbulent temperature fluctuations is significantly larger for the COSMO data than measured in previous experiments. In the present experiment strong turbulent fluctuations occurred in the lee of the model building and background atmospheric turbulence levels were large and uncontrolled. The reference data in Fig. 5b were measured in water channel or wind tunnel experiments where turbulence levels in the free stream were minimized (typically $\sigma_u/u_\infty < 5\%$). Thus the data are not expected to agree in the region $\zeta>3$.

Data from the present study were also compared with turbulence measurements in turbulent combined and turbulent forced convection WBLs, but no agreement was observed between the data so we do not include those comparisons in this paper.

4.3 Temperature timeseries and moments profiles in the wall boundary layer

Although the 30-min time averaged profiles in Fig. 5 were indicative of turbulent natural convection mode, periods of turbulent natural convection punctuated with intermittent turbulent forced convection events are apparent from a visual examination of the temperature timeseries measured in the WBL. Figs. 6a,b show a 6-sec data subset from Run #2 of temperature timeseries at various distances from the wall, and the corresponding WBL free stream velocities measured at $x = 0.9H$ and $0.78H$ respectively. When $t\text{-}t_o < 3$ s the mean streamwise velocity is constant at about 0.4 m s^{-1} and the temperature timeseries exhibit low-frequency oscillations ($f \approx 0.5\text{-}1$ Hz) consistent with the turbulent natural convection mode [9]. During $t\text{-}t_o < 3$ s three different regions of the WBL are apparent from Fig. 6a consistent with Hölling & Herwig [36].

Timeseries between $70 \leq y \leq 200$ mm are relatively constant which indicates that those measurements were made in the free stream and the thickness of the WBL at $x = 0.9H$ was approximately 70 mm. Timeseries in the outer layer away from the overlap layer $22 \leq y \leq 52$ mm exhibit random and spiky fluctuations and are uncorrelated with timeseries measured nearer to the wall, which suggests that the turbulence in the free stream influences this region of the WBL. The overlap layer $1.2 \leq y \leq 15.6$ mm is largely unaffected by the free stream but has the greatest normalized temperature standard deviation in the WBL (see Fig. 5b near $\zeta = 1$). The overlap layer was termed the buoyant sublayer (BSL) by George & Capp [37] who showed that, although the heat flux through this layer is constant, the slope of the temperature and velocity profiles in the BSL is proportional to $y^{-1/3}$. The temperature timeseries of Fig. 5a suggest that the temperature in near wall region (i.e. the conductive and thermo-viscous sublayers) was not resolved in our experiment.

At $t\text{-}t_o \approx 3$ s the mean streamwise and spanwise velocities increase rapidly to 0.8 m s^{-1}. During $t\text{-}t_o > 3$ s the temperature timeseries throughout the WBL are characterized by intermittent and spiky, peaked temperature fluctuations that are indicative of the turbulent forced convection mode [9]. At $t\text{-}t_o > 4$ s in Fig. 6a the wall surface temperature ($y = 0$ mm) decreases significantly which is consistent with increased convective heat transfer under forced convection relative to natural convection [7]. This decrease in wall temperature was not related to a change in irradiance impinging on the wall because the irradiance was relatively constant during the period shown in Fig. 6, $\langle GHI \rangle \pm \sigma_{GHI} = 581 \pm 2$ W m^{-2}.

Profiles of T' skewness and kurtosis at $0.67H$ and $0.9H$ for Runs 1 and 2 are plotted in Figs. 7a,b against the length parameter $\eta = (y/H)Gr_H^{1/4}$ after Hattori et al [10]. In the BSL ($\eta < 3$) the distribution of temperature fluctuation is nearly Gaussian (i.e. $S \approx 0$, $K \approx 3$). For turbulent natural convection, symmetric distributions of T' are expected in the BSL because the only governing parameters in that layer are Q_H and the buoyant force $g\beta$ [37] so the buoyancy driven flow in the BSL will be characterized by periodic variations of temperature. The shape of the skewness profile in Fig. 7a is similar to the observations of Hattori et al for $\eta < 3$, but the magnitude of S is smaller in our data. The shape of the kurtosis profile in Fig. 7b is also similar to the Hattori et al data but for $\eta > 1$, and the magnitude of K was smaller in our experiment. In the outer layer ($3 < \eta < 10$; consistent with the outer layer limit in Fig. 6a) the skewness becomes positive which suggests that large scale eddies intermittently eject heat away from the wall through forced

convection. In the free stream $S \approx 0$ while $K > 3.5$ indicating that the free stream temperature fluctuations were evenly distributed and the magnitude of free stream temperature fluctuation was small. These profiles are different from those of turbulent natural and combined convection [10] and provide further evidence that the BSL is decoupled from turbulent fluctuations in the free stream and the outer layer when $<u_\infty>$ is low (i.e. $<u_\infty> < \sim 0.6$ m s^{-1}).

4.4 Identification of convective modes using the continuous wavelet transform

High turbulence intensity in the free stream flow (see Figs. 4 and 5b) prevented the formation of a sustained combined convection mode in the WBL which was expected due to the existence of an aiding free stream flow. Instead natural and forced convection modes occur in a non-stationary manner because the mode of heat transfer in the WBL is controlled by wind associated with intermittent coherent structures in the UC. Continuous wavelet transforms (CWT) facilitate identification of natural and forced convection events in the non-stationary signal by resolving different scales of variability contained in the input signal as a function of time [38]. The CWT was applied to the temperature timeseries measured at y = 3.6 mm (previously determined to be inside the BSL) using the Haar function as the parent wavelet. The Haar wavelet (ψ) and the associated scaling function (φ) are

$$\psi(t) = \begin{cases} 1, & t \in (0., 0.5] \\ -1, & t \in (0.5, 1] \\ 0. & \text{otherwise} \end{cases} \text{ and} \qquad (4a)$$

$$\varphi(t) = \begin{cases} 1, & t \in (0., 1] \\ 0. & \text{otherwise} \end{cases}. \qquad (4b)$$

The Haar wavelet has several desirable properties that make it useful for the detection of heat transfer modes in the context of our experiment. $\psi(t)$ has a periodic shape which is useful for detecting periodic oscillations in the input signal that are the characteristic signature of the natural convection mode. $\psi(t)$ is termed a "first derivative-like" wavelet because the Fourier transform $\hat{\psi}(\omega)$ is proportional to $i\omega$ where $i = (-1)^{1/2}$ and ω is the frequency. Thus $\psi(t)$ is also useful for detecting discontinuities in the first derivative of an input signal under a CWT. Such discontinuities occur during forced convection events, which are shaped like sharp peaks and occur intermittently in the BSL temperature timeseries. Finally $\psi(t)$ is well localized in time which enables precise detection of discontinuities and other phenomena in time [38].

Characteristic CWTs of turbulent natural and forced convection events are presented in Fig. 8 along with plots of the corresponding temperature timeseries at y = 3.6 mm and UC wind

velocity. In Figs. 8a-c the turbulent natural convection mode occurs during the range $2 < t\text{-}t_o < 7$ s. During that period the temperature timeseries of Fig. 8b exhibits oscillatory behaviour with a regular period. This phenomenon is captured in the CWT as a grouping of four local maxima and minima in the wavelet coefficient C_g that are confined to small scales $20 < 1/a < 80$, where $1/a$ is the dimensionless scale factor. C_g is representative of the correlation between the input signal $h(t)$ and the parent wavelet $\psi(t)$. Large magnitude values of C_g indicate high correlation or anti-correlation between $h(t)$ and $\psi(t)$ for positive and negative C_g respectively. Figure 8c shows that the UC wind velocities were less than 0.6 m s^{-1} during this natural convection event. The characteristic frequency of this natural convection event was $f_n \approx 1.1$ Hz which was determined from the average spacing of the local maxima in Fig. 8a; of course f_n will vary in the same sense as Gr_H.

In Figs. 8d-f the turbulent forced convection mode occurs over the entire data subset. The temperature timeseries of Fig. 8e is characterized by intermittent, sharp peaks that lag increases in the streamwise velocity by about 1 s. These forced convection events are captured in the CWT as long streaks that extend through all scales $1/a > 20$. It is apparent from Fig. 8d that forced convection events are caused by gusts in the free stream velocity (u and w) and occur intermittently in the temperature timeseries. It is relevant to note that these events were detected from CWT plot and then the mode of convection was confirmed by visual examination of the temperature timeseries and UC wind velocity. Thus it appears that the CWT using the Haar wavelet is an appropriate method to identify the mode of heat transfer in the turbulent WBL.

4.5 Comparison of COSMO heat flux to existing wall functions

Operating under the assumption that the temperature measurement closest to the wall at $y = 1.2$ mm is near the boundary of the thermo-viscous sublayer (VSL; see Section 5 for discussion) we attempt to compute the sensible heat flux at the wall from $Q_H = -\lambda(\partial T/\partial y)|_{y=0}$ [7]. Average heat transfer parameters for the COSMO experiment are presented in Table 2 along with Nu_H values computed for each run and measurement location using four independent but equivalent WFs for convective heat transfer on outdoor, leeward, vertical surfaces; Loveday & Taki [2], Sharples [39], ASHRAE/DOE-2 [40] and Test et al [41]. During both runs Gr_H is larger at $x = 0.9H$ compared to $x = 0.67H$ because T_S is greater at the upper location due to heat conduction through the roof of the model building. Because the shape of $T(y)$ is concave up, poor spatial resolution of temperature measurements in the VSL will cause the magnitude of $(\partial T/\partial y)|_{y=0}$ to be

underestimated so the heat flux values for COSMO in Table 2 are expected to be smaller than the true values. The WFs proposed by Loveday & Taki, Sharples and ASHRAE all significantly underestimate Nu_H. Poor agreement is observed between these models and the COSMO data, and among the models themselves. The values of Nu_H computed using the Test et al model are similar to the values computed from the COSMO data.

5. Discussion

Based on the Patel et al [13] simulations the expected flow regime in our experiment was transitional combined convection, but the Hattori et al [9] data suggested laminar combined convection flow. Both of these predictions were inconsistent with our measurements that clearly indicated the existence of turbulent flow in the WBL. The transition to turbulence in BLs is strongly related to the amount of turbulence in the free stream [20]. The initial transition to turbulence in the Patel et al study was forced to occur at threshold values of Re and Gr that were selected based on the experiments of Black and Norris [42]. Hattori et al [9] used a carefully designed wind tunnel with very low free stream turbulence to measure the value of Gr for transition to turbulence. For the present study it is likely that turbulence in the free stream and/or wall roughness caused bypass transition to turbulence so laminar and transitional flow regimes were not encountered.

The dimensionless length parameter ζ has been used by many authors to correlate temperature data in turbulent natural convection BLs for the inner layer as well as the entire BL region [3]. Our decision to use ζ as a length parameter in Section 4.2 was primarily based on the ease of comparison with existing data. Cheesewright and Mirzai [43] stressed that mean temperature profiles from experiments in different fluids (e.g. air and water) can be well correlated using ζ as the length parameter up to $Gr < \sim 10^{13}$. This claim is supported by the close agreement observed among the profiles from previous experiments plotted in Figs. 5a,b. However, it is important to note that the length parameter ζ is obtained from scaling y by the slope of the temperature profile within the VSL, a quantity which could not be calculated accurately from the COSMO data since the viscous region of the WBL was not resolved (see Figs. 5 and 6). This calls into question the validity of the comparison between the profiles since there is uncertainty in the values of ζ computed from the COSMO data which cannot be quantified. We expect that lack of resolution of the temperature profile in VSL will cause any

estimate of $(\partial\theta/\partial y)|_{y=0}$ to be larger (less negative) than the true value since the profile $\theta(y)$ has negative slope and concave upward shape. Because ζ is directly proportional to $-(\partial\theta/\partial y)|_{y=0}$ (and a constant value of $<\partial\theta/\partial y|_{y=0}>$ is assumed over each run) poor resolution in the VSL should cause ζ to be underestimated and data from the present study to be shifted leftward in Fig. 5a relative to data from previous experiments. That all the profiles in Fig. 5a are well correlated and a leftward shift of our data is not observed in Fig. 5a leads to the conclusion that the temperature measurement nearest the wall in the WBL was just outside the boundary of the VSL so that only a small bias was introduced in ζ. Thus good agreement between previous measurements of WBL temperature profiles and profiles from the present study indicates that the dominant mode of heat transfer in the WBL flow observed in COSMO was turbulent natural convection. The foregoing argument also justifies the convective heat flux calculations presented in Section 4.5.

The result that turbulent natural convection was the dominant heat transfer mode in the WBL was unexpected because it suggests that in dense urban areas ($H/S \geq 0.7$; [21]) winds in the UC do not contribute significantly to heat transfer on the leeward walls. However, our data were obtained in a 1/5 scale urban model where velocity and length scales for the WBL Reynolds number were taken as u_∞ and H respectively. If these scales are translated to a real city then Re will be five times that observed in COSMO (assuming similar wind conditions in the UC). The Grashof number is proportional to H^3 so for full scale buildings building the Gr is expected to become much greater than $O(10^9)$ even when T_S-T_∞ is only a few degrees Celsius.

The implication of this scaling argument is that, on a full-scale building wall, the transition from turbulent natural to turbulent combined convection is certain to occur in the leeward WBL. Under turbulent combined convection the heat flux between the wall and the air is suppressed when compared with heat flux in turbulent natural or forced regimes [8], [9]. Under moderately windy conditions the convective heat transfer coefficient (and consequently convective cooling) of leeward building walls in dense urban areas may be reduced relative to high wind conditions, when increased canyon wind speeds would result in forced convection (Fig. 4). This finding is relevant to urban design because it suggests that it is advantageous to increase the width of street canyons so that wake-interference flow is realized in the RSL (specify $H/S < 0.7$; [21]). This would not only reduce surface temperatures due to radiative effects (i.e. increased sky view factor for urban surfaces) but also increase convective cooling on leeward building walls (and

reduce overall building cooling load) by preventing the development of combined mode convective flow.

The analysis presented in Sections 4.3 and 4.4 indicates that the structure of the WBL is intermittent. Although on average temperature profiles in the WBL assume a form similar to those in turbulent natural convection (see Fig. 5), CWTs of temperature timeseries in the BSL reveal the occurrence of a many turbulent forced convection events and periods during which the boundary layer structure is transitional. This intermittent structure can be explained by the intermittent nature of the UC winds. Our observations indicate that existing wind tunnel heat transfer correlations obtained for turbulent natural, combined and forced convection regimes are not applicable in their current form to leeward building walls in dense urban areas.

Existing WFs that were developed from energy balance experiments cannot accurately predict Q_H on leeward walls because they compensate for the intermittent structure of the WBL with long time averages of measured data. The shortcomings of this type of WF are apparent from the data presented in Section 4.5, Table 2 that show large differences between values of Nu_H computed using four similar WFs designed for outdoor, leeward, vertical walls. Good agreement between Nu_H computed from the COSMO data and the Test et al [41] WF are attributed to the unique experimental method employed in the Test et al study which produced conditions that were similar to our experiment. Unlike the other WFs applied in Table 2, the Test et al WF is modelled from data collected on the leeward surface of a 1.2x0.81x0.20 m vertically oriented plate mounted outside under real atmospheric conditions and Test et al did not limit their data by wind direction. These conditions are similar to our experiment because complex, turbulent winds in the UC caused variable direction of the WBL free stream flow. In contrast both Loveday & Taki [2] and Sharples [39] conducted measurements on walls of isolated, full-scale buildings. In those studies data were limited according to wind direction such that an incidence angle of ±90˚ relative to the normal of the leeward wall was required for data to be used in the formulation of leeward WFs. The Test et al WF is most applicable to our study since the experimental model and atmospheric conditions are similar in both cases. Pedersen et al [40] took a rather convoluted approach to develop the ASHRAE/DOE-2 WF by combining WFs from different outdoor experiments in a power law relationship. It is worth noting that the increased complexity of the ASHRAE/DOE-2 WF does not appear to provide improved accuracy when compared with the other WFs in Table 2. The poor agreement between the WFs applied in

Table 2 also suggests that those formulations do not preserve scale similarity between models and full scale buildings.

6. Conclusion

The flow regime of a convective WBL on a vertical, leeward building wall in a 1/5 scale outdoor model of an urban area was studied experimentally using direct measurements of turbulent temperature fluctuations in the WBL and wind speed in and above the UC. Our findings underscore the need to develop consensus regarding appropriate WFs for convection on vertical surfaces in urban environments and collect more data that can be applied to validate urban computational fluid dynamics codes. From data analysis and comparison to previous experiments we draw the following conclusions about the structure of the outdoor, vertical WBL:

- Existing WBL flow regime classifications (as a function of *Gr* and *Re*) developed for convective WBL flows in controlled experiments were not consistent with our observations of the WBL in an outdoor urban environment. Turbulent natural convection was observed on the leeward building wall for relatively low values of *Gr* and *Re* when compared with wind tunnel and water channel experiments.
- The mode of heat transfer in the leeward WBL is intermittent which is problematic for developing universally applicable WFs. This fact also suggest that existing engineering heat transfer correlations that do not account for the intermittent structure of the WBL flow are not appropriate in urban environments.
- Our results suggest that decreasing the ratio *H/S* in cities located in warm climates has the potential to increase convection on leeward building walls, thus reducing overall building cooling load.

Acknowledgements

The authors wish to acknowledge the invaluable contributions of Messrs. Hiroshi Takimoto, Makoto Nakayoshi, Hideaki Kumemura and Takuya Makabe who helped design and setup the experiment. Without their advice and expertise this study would not have been possible. Discussions with Mr. Anirban Garai helped to develop the analysis presented in this paper. Funding was provided by the National Science Foundation (NSF) and the Japan Society for the Promotion of Science (JSPS) through the East Asia and Pacific Summer Institutes (EAPSI)

program. Inagaki was supported by a Ministry of Education, Science, Sports and Culture – Japan, Grant-in-Aid for Young Scientist (B): 21760382. Kleissl was supported by a NSF CAREER award.

References

[1] G.M. Mills and A.J. Arnfield, Simulation of the energy budget of an urban canyon – II. Comparison of model results with measurements, *Atmospheric Environment* **27B**(2) (1993) 171-181.

[2] D.L. Loveday and A.H. Taki, Convective heat transfer coefficients at a plane surface on a full-scale building façade, *Int. J. Heat Mass Transfer* **39**(8) (1996) 1729-1742.

[3] X. Yuan, A. Moser, P. Suter, Wall functions for numerical simulation of turbulent natural convection along vertical plates, *Int. J. Heat Mass Transfer* **36**(18) (1993) 4477-4485.

[4] S.B. Pope, Turbulent Flows, Cambridge University Press, Cambridge, 2000, pp. 335-336.

[5] R. Cheesewright, Natural convection from a vertical plane surface, PhD thesis, University of London, London, UK, 1966.

[6] R. Cheesewright, Turbulent natural convection from a vertical plane surface, *J. Heat Transfer* **90**(1) (1968) 1-8.

[7] T. Tsuji and Y. Nagano, Characteristics of a turbulent natural convection boundary layer along a vertical flat plate, *Int. J. Heat Mass Transfer* **31**(8) (1988) 1723-1734.

[8] K. Kitamura and T. Inagaki, Turbulent heat and momentum transfer of combined forced and natural convection along a vertical flat plate – aiding flow, *Int. J. Heat Mass Transfer* **30**(1) (1987) 23-41.

[9] Y. Hattori, T. Tsuji, Y. Nagano, N. Tanaka, Characteristics of turbulent combined-convection boundary layer along a vertical heated plate, *Int. J. Heat Fluid Flow* **21** (2000) 520-525.

[10] Y. Hattori, T. Tsuji, Y. Nagano, N. Tanaka, Effects of freestream on turbulent combined-convection boundary layer along a vertical heated plate, *Int. J. Heat Fluid Flow* **22** (2001) 315-322.

[11] P.H. Oosthuizen, Turbulent combined convection flow over a vertical plane surface, *Proc. 5th Int. Heat Transfer Conf.* **3** (1974) 129-133.

[12] T.S. Chen, B.F. Armaly, M.M. Ali, Turbulent mixed convection along a vertical plate, *J. Heat Transfer* **109**(1) (1987) 251-253.

[13] K. Patel, B.F. Armaly, T.S. Chen, Transition from turbulent natural convection to turbulent forced convection, *J. Heat Transfer* **120**(4) (1998) 1086-1089.

[14] W.P. Jones and B.E. Launder, The prediction of laminarization with a two-equation model of turbulence, *Int. J. Heat Mass Transfer* **15** (1972) 301-314.

[15] W. Nusselt and W. Jürges, Die Kühlung einer ebenen Wand durch einen Luftstrom (The cooling of a plane wall by an air flow), *Gesundheits Ingenieur* **52**(45) (1922) 641-642 (In German).

[16] A. Hagishima and J. Tanimoto, Field measurements for estimating the convective heat transfer coefficient at building surfaces, *Build. Environ.* **38** (2003) 873-881.

[17] J. Henmi, K. Narita, N. Sawachi, H. Seto and Y. Ishikawa, Real scale measurement of convective heat transfer coefficient on vertical building wall, *Proc. 73rd Architectural Research Meetings*, Kanto Chapter, Architectural Institute of Japan (2002) 676-678 (In Japanese).

[18] R.J. Cole and N.S. Sturrock, The convective heat exchange at the external surface of buildings, *Build. Environ.* **12**(4) (1977).

[19] J.A. Palyvos, A survey of wind convection coefficient correlations for building envelope energy systems modeling. *Appl. Therm. Eng.* **28** (2008) 801-808.

[20] H. Schlichting, Boundary-layer Theory 7th ed., Mcgraw-Hill, New York, 1979, pp. 415-419.

[21] T.R. Oke, Boundary Layer Climates, 2nd ed., Routledge, New York, 1987, pp. 464.

[22] I.P. Castro an d A.G. Robins, The flow around a surface-mounted cube in uniform and turbulent streams, *J. Fluid Mech.* **79**(2) (1977) 307-335.

[23] H.J. Hussein and R.J. Martinuzzi, Energy balance for turbulent flow around a surface mounted cube placed in a channel, *Phys. Fluids* **8**(3) 764-780.

[24] E.R. Meinders, Experimental study of heat transfer in turbulent flows over wall-mounted cubes. Ph.D. Thesis, Faculty of Applied Sciences, Delft University of Technology, Delft, Netherlands, 1998, pp. 279.

[25] S. Onomura, H. Takimoto, M. Kanda, Influence of a heated wall on urban canopy flow using PIV measurements, Seventh International Conference on Urban Climate (ICUC), Yokohama, Japan, 2009.

[26] H.J.S. Fernando, D. Zajic, S. Di Sabatino, R. Dimitrova, B. Hedquist, A. Dallman, Flow, turbulence, and pollutant dispersion in urban atmospheres, *Phys. Fluids* **22**, 051301 (2010).

[27] E.R. Meinders and K. Hanjalić, Vortex structure and heat transfer in turbulent flow over a wall-mounted matrix of cubes, *Int. J. Heat Fluid Flow* **20** (1999) 255-267.

[28] A. Inagaki and M. Kanda, Turbulent flow similarity over an array of cubes in near-neutrally stratified atmospheric flow, *J. Fluid Mech.* **615** (2008) 101-120.

[29] H. Cheng and I.P. Castro, Near wall flow over urban-like roughness, *Boundary-Layer Met.* **104** (2002) 229-259.

[30] P.T. Tsilingiris, Thermophysical and transport properties of humid air at temperature range between 0 and 100 degC, *Energy Conversion and Management* **49** (2008) 1098-1110.

[31] C.J. Fraser, D. Graham, J.S. Milne, Digital processing of hot wire anemometer signals in intermittently turbulent flows, *Flow Meas. Instrum.* **1** (1990) 225-325.

[32] A.S. Thom, Momentum absorption by vegetation, *Quart. J. R. Met. Soc.* **97** (1971) 414-428.

[33] P. Louka, S.E. Belcher, R.G. Harrison, Coupling between air flow in streets and the well-developed boundary layer aloft, *Atmos. Environ.* **34** (2000) 2613-2621.

[34] M. Miyamoto, H. Kajino, J. Kurima, I. Takanami, Streamwise developments of turbulent characteristics in a vertical free convection boundary layer, *Proc. 18th National Heat Transfer Symposium of Japan*, Sendai (1981) 295-298.

[35] R.R. Smith, Characteristics of turbulence in free convection flow past vertical plate, PhD thesis, University of London, London, UK, 1972.

[36] M. Hölling and H. Herwig, Asymptotic analysis of the near-wall region of turbulent natural convection flows, *J. Fluid Mech.* **541** (2005) 383-397.

[37] W.K. George and S.P. Capp, A theory for natural convection turbulent boundary layers next to heated vertical surfaces, *Int. J. Heat Mass Transfer* **22** (1979) 813-826.

[38] S. Collineau and Y. Brunet. Detection of turbulent coherent motions in a forest canopy Part 1: Wavelet analysis, *Boundary-Layer Meteorology* **65** (1993) 357-379.

[39] S. Sharples, Full-scale measurements of convective energy losses from exterior building surfaces, *Build. Environ.* **19** (1984) 31-39.

[40] C.O. Pedersen, R.J. Liesen, R.K. Strand, D.E. Fisher, L. Dong, P.G. Ellis, A toolkit for building load calculations; Exterior heat balance (CD-ROM), *American Society of Heating, Refrigerating and Air Conditioning Engineers (ASHRAE), Building Systems Laboratory* (2001).

[41] F.L. Test, R.C. Lessmann, A. Johary, Heat transfer during wind flow over rectangular bodies in the natural environment, *J. Heat Transfer* **103** (1981) 262-267.

[42] W.Z. Black and J.K. Norris, The thermal structure of free convection turbulence from inclined isothermal surfaces and its influence on heat transfer, *Int. J. Heat Mass Transfer* **18**(1) (1975) 43-50.

[43] R. Cheesewright and M.H. Mirzai, The correction of experimental velocity and temperature data for a turbulent natural convection boundary layer, *U.K. Natn. Conf. on Heat Transfer*, Glasgow, 1988, 79-89.

Figure Captions

Figure 1 – Plan view schematic of the COSMO facility. The squares indicate 1.5 m concrete cubes. The experiment was set-up in the canyon marked 'x' and measurements were taken on the wall of the adjacent building (shaded square). Met towers (triangles) prevented locating the experiment on the NW-SE axis. The predominant wind was from the SE.

Figure 2 – A schematic drawing of the experimental setup. The predominant wind in the surface layer was in the X direction.

Figure 3 – Flow regime maps for vertical turbulent and natural convection WBLs generated from **(a)** numerical experiments (re-plotted from [13]) and **(b)** wind tunnel data (taken from [9]). The red box indicates the range of Gr and Re observed in the present study.

Figure 4 – Scatter plot illustrating the relationship between the horizontal wind speed at $2H$ and the average vertical velocity on the leeward wall of the canyon (measured at $0.78H$). Angle brackets denote a 1-min time average and vertical error bars indicate the magnitude of the UC wind speed standard deviation within each minute.

Figure 5 – Dimensionless profiles of **(a)** mean temperature and **(b)** normalized temperature standard deviation in a turbulent natural convective WBL plotted against the length parameter ζ. Black points are data reported from previous experiments and data from the present study is plotted in red. Figures re-plotted from refs. [7], [34] and [35].

Figure 6 – A six second data subset from Run #2 showing **(a)** temperature timeseries in the WBL measured at height $x = 0.9H$ and **(b)** free stream wind velocities in the UC measured at $x = 0.78H$.

Figure 7 – Profiles of **(a)** skewness and **(b)** kurtosis in the WBL for Run #1 and #2. Expected values for a Gaussian distribution are marked as horizontal lines.

Figure 8 – Representative CWTs with corresponding temperature timeseries (measured at $x = 0.9H$, $y = 3.6$ mm) and wind velocity in the UC (measured at $x = 0.78H$) for **(a-c)** the turbulent natural convection mode (Run #1) and **(d-f)** the turbulent forced convection mode (Run #2). In Figs. 8a,d a is the dimensionless scale factor and the colour scale is the magnitude of the wavelet coefficient C_g.

Table Captions

Table 1 – Atmospheric conditions during two 30 minute sampling periods. Angle brackets denote a time averaged quantity.

Table 2 – Time averaged values of heat transfer parameters computed from the COSMO data and Nu_H for the vertical wall computed using four different wall functions for convective heat transfer on leeward, vertical, urban surfaces.

Suggested Placement of Figures and Tables (in chronological order)

Figure 1 to be placed before the first paragraph of Section 2.1

Figure 2 to be placed after the first paragraph of Section 2.2

Figure 3 to be placed before the first paragraph of Section 2.4

Figure 4 to be placed after the second paragraph of Section 4.1

Figure 5 to be placed near the first paragraph of Section 4.2

Figure 6 to be placed after the second paragraph of Section 4.3

Figure 7 to be placed at the end of Section 4.3 before Section 4.4

Figure 8 to be placed in or near Section 4.4

Table 1 to be placed after the heading for Section 3

Table 2 to be placed at the beginning of Section 4.5

Figure 1

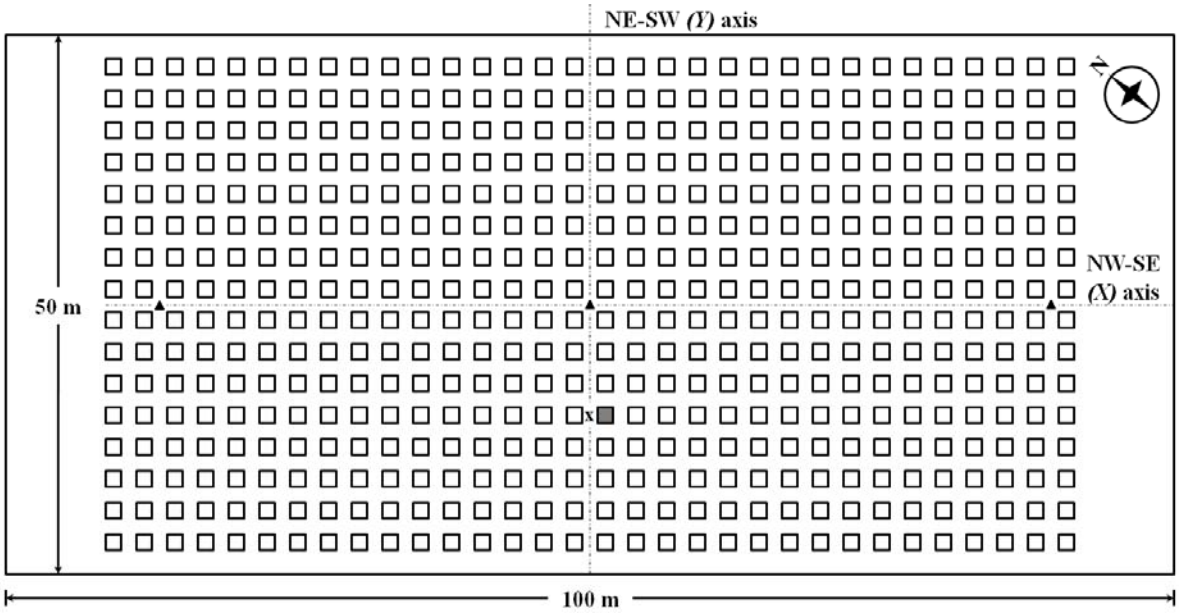

Figure 2

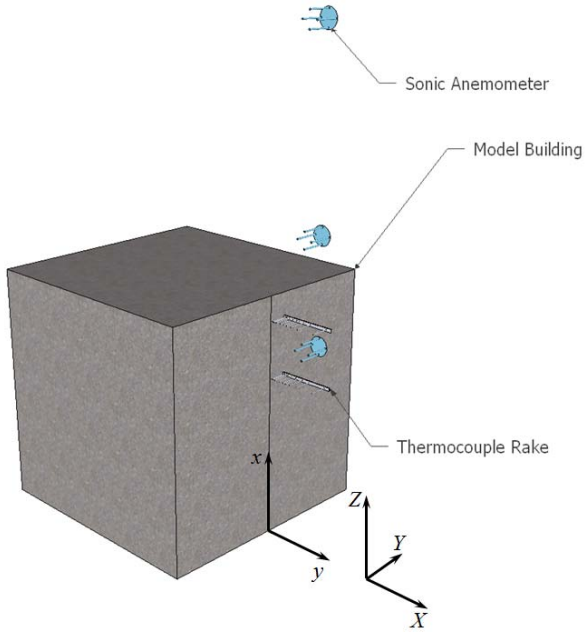

Figure 3

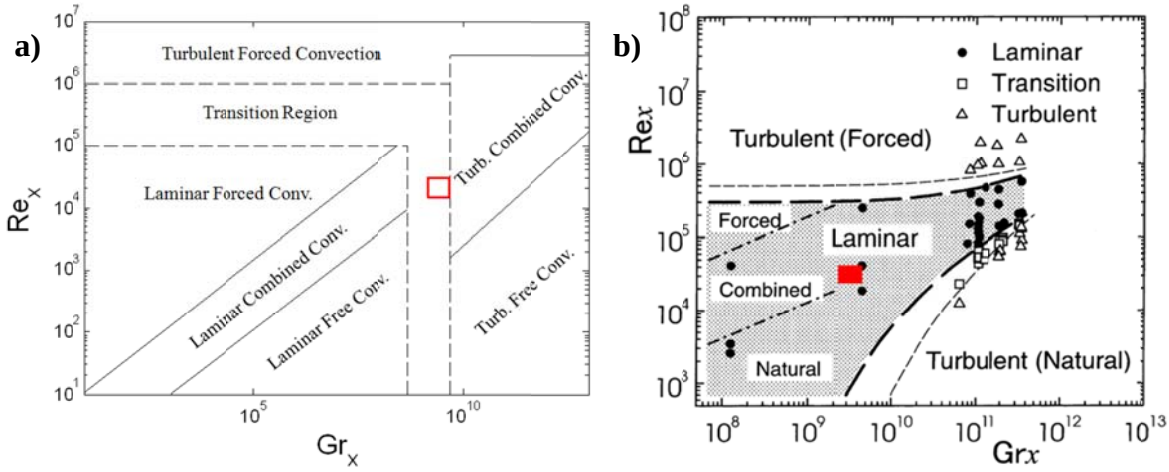
a)
Turbulent Forced Convection
Transition Region
Laminar Forced Conv.
Laminar Combined Conv.
Laminar Free Conv.
Turb. Combined Conv.
Turb. Free Conv.
Re_X
Gr_X
b)
Laminar
Transition
Turbulent
Turbulent (Forced)
Forced
Laminar
Combined
Natural
Turbulent (Natural)
Rex
Grx

Figure 4

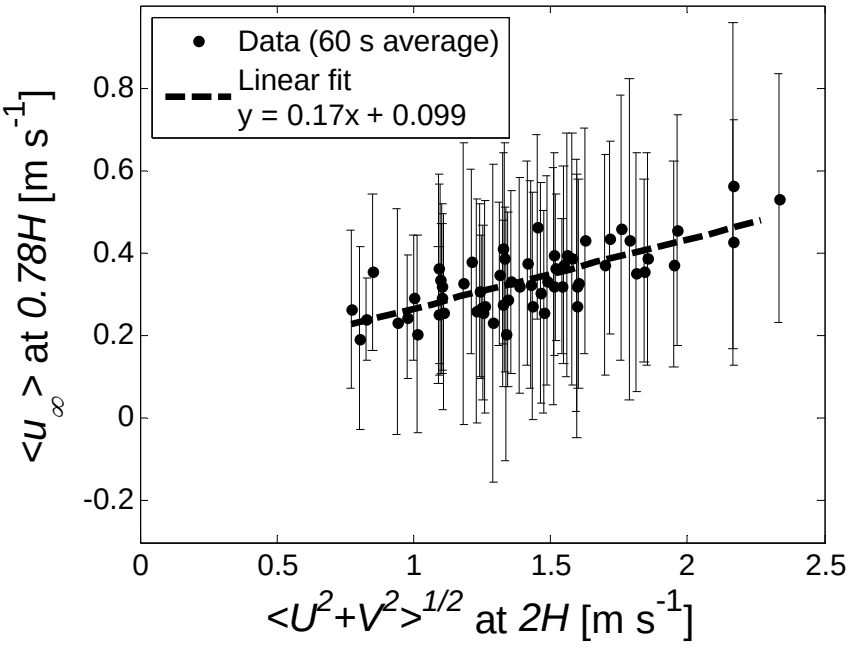
Data (60 s average)
Linear fit
y = 0.17x + 0.099
0.8
0.6
0.4
0.2
0
-0.2
0
0.5
1
1.5
2
2.5
<u∞> at 0.78H [m s-1]
<U2+V2>1/2 at 2H [m s-1]

Figure 5

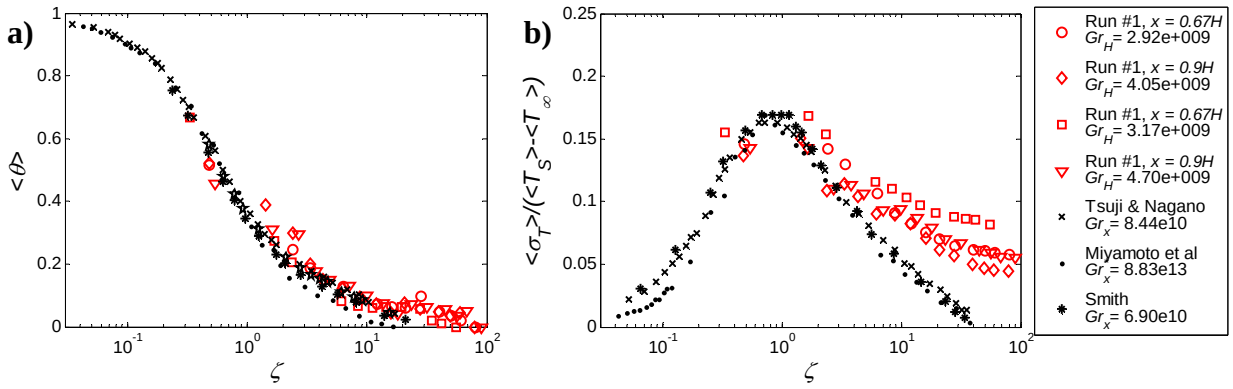
a)
b)
<θ>
<σT>/(<TS>-<T∞>)
ζ
ζ
Run #1, x = 0.67H
GrH= 2.92e+009
Run #1, x = 0.9H
GrH= 4.05e+009
Run #1, x = 0.67H
GrH= 3.17e+009
Run #1, x = 0.9H
GrH= 4.70e+009
Tsuji & Nagano
Grx= 8.44e10
Miyamoto et al
Grx= 8.83e13
Smith
Grx= 6.90e10

Figure 6

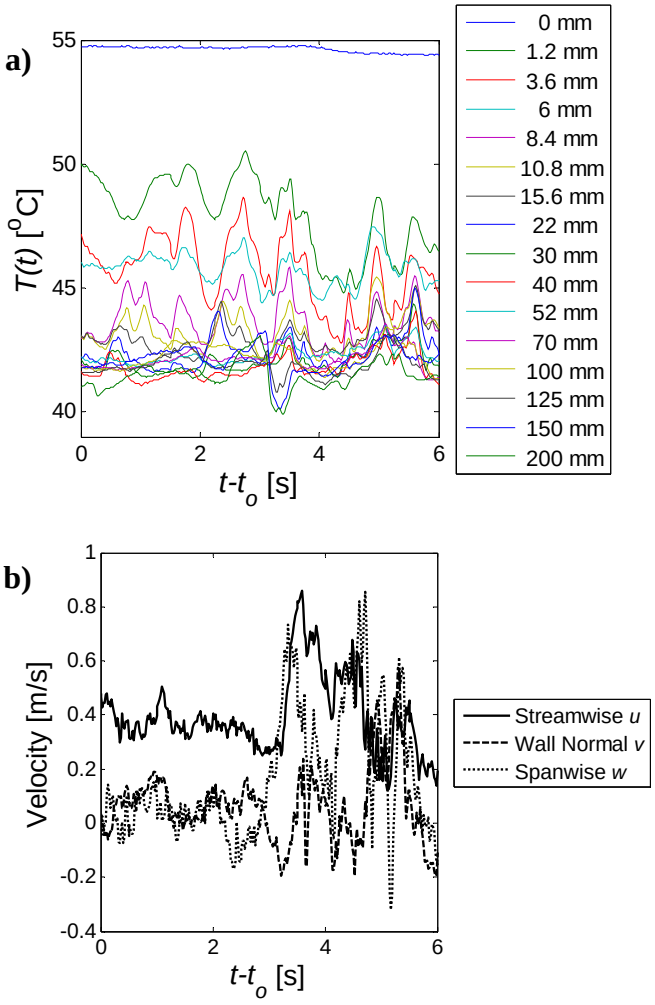
a)
55
50
45
40
T(t) [°C]
0
2
4
6
t-t_o [s]
0 mm
1.2 mm
3.6 mm
6 mm
8.4 mm
10.8 mm
15.6 mm
22 mm
30 mm
40 mm
52 mm
70 mm
100 mm
125 mm
150 mm
200 mm
b)
1
0.8
0.6
0.4
0.2
0
-0.2
-0.4
Velocity [m/s]
0
2
4
6
t-t_o [s]
Streamwise u
Wall Normal v
Spanwise w

Figure 7

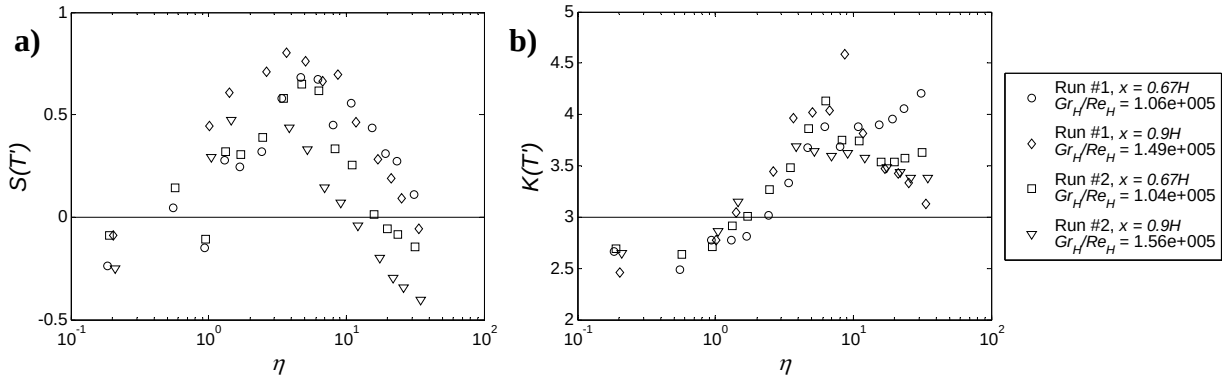
a)
b)
S(T')
K(T')
η
η
Run #1, x = 0.67H
Gr_H/Re_H = 1.06e+005
Run #1, x = 0.9H
Gr_H/Re_H = 1.49e+005
Run #2, x = 0.67H
Gr_H/Re_H = 1.04e+005
Run #2, x = 0.9H
Gr_H/Re_H = 1.56e+005

Figure 8

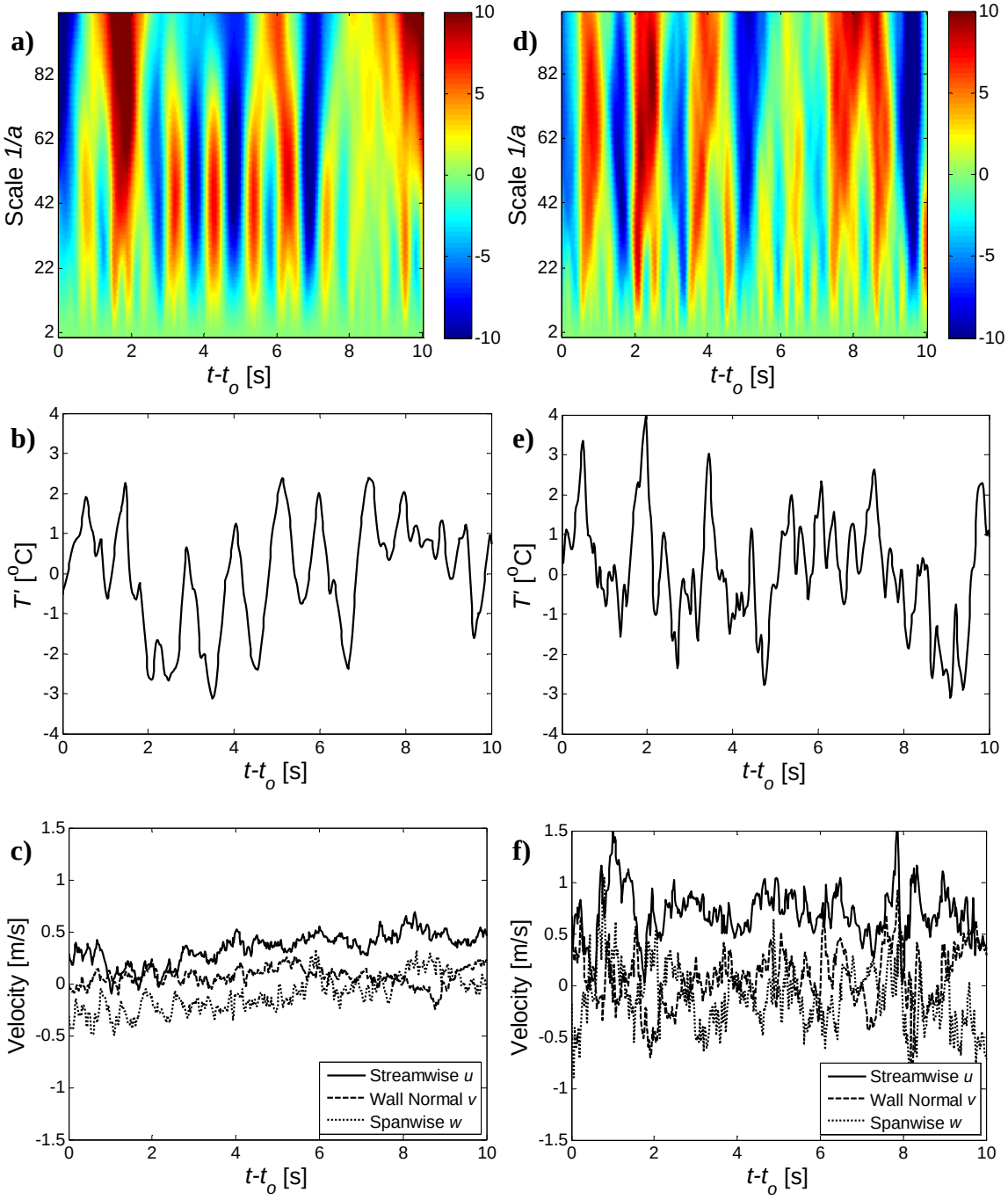
a)
d)
Scale 1/a
82
62
42
22
2
0
2
4
6
8
10
t-t_o [s]
10
5
0
-5
-10
b)
e)
T' [°C]
4
3
2
1
0
-1
-2
-3
-4
c)
f)
Velocity [m/s]
1.5
1
0.5
0
-0.5
-1
-1.5
Streamwise u
Wall Normal v
Spanwise w

Table 1

Date	**Run**	**$\langle(U^2+V^2)^{1/2}\rangle$ [m s^{-1}]**	**$\langle u_\infty \rangle$ [m s^{-1}]**	**Z_{eff} [m]**	**$\xi = Z_{eff}/L$**	***Ri***
7/22/2010	#1	1.26 ± 0.50	0.31 ± 0.25	1.7	-0.17	-0.22
7/23/2010	#2	1.56 ± 0.60	0.36 ± 0.28	1.7	-0.21	-0.29

Table 2

Run	x	$\langle Q_H \rangle$ COSMO [W m^{-2}]	$\langle h_o \rangle$ COSMO [W m^{-2} K^{-1}]	$\langle Gr_H \rangle$ *COSMO*	$\langle Re_H \rangle$ COSMO	$\langle Nu_H \rangle$ COSMO	$\langle Nu_H \rangle$ Loveday	$\langle Nu_H \rangle$ Sharples	$\langle Nu_H \rangle$ ASHRAE/ DOE-2	$\langle Nu_H \rangle$ Test
#1	0.67H	87	11	3.0×10^9	2.8×10^4	610	370	230	290	620
	0.90H	120	11	4.1×10^9	2.8×10^4	600	370	230	300	620
#2	0.67H	68	7.5	3.2×10^9	3.1×10^4	420	400	240	320	660
	0.90H	170	12	4.8×10^9	3.0×10^4	680	400	240	330	650